

## NOTES AND CORRESPONDENCE

**Potential Vorticity Structure across the Gulf Stream: Observations and a PV-Gradient Model**

OLEG LOGOUTOV, GEORGE SUTYRIN, AND D. RANDOLPH WATTS

*Graduate School of Oceanography, University of Rhode Island, Narragansett, Rhode Island*

6 August 1999 and 17 July 2000

## ABSTRACT

Potential vorticity (PV) structure across a baroclinic front is a property that determines the stability characteristics of that front, cross-frontal exchange, and the behavior of the vortical waves that this front enables. Hence, there has been much interest in estimating PV across the Gulf Stream (GS). However, PV estimations have typically encountered two problems—the horizontal resolution of sampling has been inadequate, and noise in measurements gets amplified by differentiation when estimating PV. This paper's approach addresses both of these problems.

The authors have used a unique set of highly resolved, simultaneous density and direct velocity measurements across the Gulf Stream, first to calculate the PV structure, and then to obtain its idealization within density layers using a PV-gradient (PVG) model. The PVG model inverts an input PV in layers to determine the isopycnal depths and velocities in isopycnal layers. By comparing the observed and PVG-modeled velocities and isopycnal positions, corrections to PV estimates can be made to improve agreement. In this way an idealized and smooth PV-gradient structure can be obtained that is dynamically consistent with the velocity and density fields and retains the correct magnitudes of the PV gradients while noise and insignificant details are filtered out.

The GS PV structure can be successfully idealized as a "3-PVG-layer" representation, which has a strong positive PV gradient in the 18°C Water layer, a weak positive PVG in the upper main thermocline, and a weak negative PVG in the lower main thermocline. The associated velocity structure captures the core velocity throughout the upper main thermocline, the width, the vertical tilt, and the asymmetry of the flow with higher lateral shear on the cyclonic side.

**1. Introduction and background**

Estimates of the potential vorticity (PV) structure across the Gulf Stream (GS) are employed in many analytical and numerical studies. First, the PV structure across a baroclinic front is a key element controlling the stability properties of that front (Killworth 1980; Boss et al. 1996). Second, the horizontal PV gradient provides a restoring force for the mean-flow trapped waves (Bane 1980) and is crucial in determining their dispersion characteristics and modal structure. Third, the cross-frontal exchange processes are dependent on the cross-stream PV distribution (Lozier and Bercovici 1992; Bower and Lozier 1994). Last, a class of numerical and analytical models requires PV for initialization (e.g., Pratt and Stern 1986; Sutyryn and Yushina 1989; Pratt et al. 1991; Meacham 1991; Boss et al. 1996). All these reasons give a strong motivation to the

attempts to obtain realistic but smooth PV estimates across the Gulf Stream and to find the proper values of the cross-frontal PV gradients in different Gulf Stream layers.

Historically, the study of the Gulf Stream PV has begun with a 1.5-layer representation discussed in Stommel (1965). Following an argument that the subtropical gyre provides source waters for the Gulf Stream, and based on observations that the PV (estimated as  $f/D_0$ , where  $D_0$  is the depth of the 10° isotherm) remains nearly constant over the western sector of the gyre, Stommel assumed homogeneous PV on the anticyclonic side of the Gulf Stream and pictured the Gulf Stream PV structure as an abrupt front of zero width.

Estimates of the GS PV based on direct velocity and CTD measurements were given by Watts (1983) and Johns (1984). The latter argues that the realistic Gulf Stream PV structure should be characterized by division into at least four vertical zones: the surface layer (<250 m depth), the 18° Water layer, the main thermocline, and the deep water layer underneath the main thermocline.

Isopycnal estimates of the GS PV were described in

---

*Corresponding author address:* Mr. Oleg G. Logoutov, Graduate School of Oceanography, Box 200, University of Rhode Island, Narragansett, RI 02882-1197.  
E-mail: ologoutov@gso.uri.edu

Bower et al. (1985), Leaman et al. (1989), Liu and Rossby (1993), Hall and Fofonoff (1993), and Hall (1994). Important advantages of analyzing PV in an isopycnal framework were pointed out for analogous atmospheric studies by Hoskins et al. (1985). First, the PV and potential density are both approximately conserved in fluid parcels when advective processes dominate frictional and diabatic ones. Second, if the total mass within each isopycnal layer is specified, then a knowledge of the global PV distribution on each isopycnal surface is sufficient to deduce, diagnostically, all other dynamical fields (such as pressure, velocity, and density) under suitable balance conditions.

Previous studies have made various assumptions about the Gulf Stream velocity or density structure. Bower et al. (1985) estimated PV using the Gulf Stream '60 survey data (station spacing about 50 km) neglecting the relative vorticity parts. Leaman et al. (1989) provided PV estimates using temperature as a proxy to the GS density field. A similar approach was used by Hall (1994) who had applied Hendry's model to expendable bathythermograph data. Hall and Fofonoff (1993) have used the geostrophic approximation to the GS velocity field with the barotropic component taken from earlier studies.

In broad-brush description, isopycnal PV estimates increase sharply at the cyclonic edge in densities above  $\sigma_\theta \approx 27.1$  ( $\theta \approx 11^\circ\text{C}$ ). This increase reflects the front between weakly stratified Sargasso Sea water and more strongly stratified slope waters, and a sharp gradient in relative vorticity at these depths. Along the  $\sigma_\theta \approx 27.5$  ( $\theta \approx 7^\circ\text{C}$ ) and deeper isopycnals the PV is usually pictured as relatively uniform, which suggests that water parcels have little trouble mixing across the Gulf Stream front at these lower depths. This basic PV structure was also confirmed by float observations in the Gulf Stream (Lozier and Bercovici 1992; Bower and Lozier 1994).

## 2. Our goals, data, and methods

The goal of this study is to find a simplified but realistic and dynamically consistent model of the PV structure across the Gulf Stream and to provide robust estimates to the cross-frontal PV gradients in different layers. Previous attempts to estimate cross-frontal PV from observations have typically encountered two problems: inadequacy of horizontal resolution and measurement noise, which gets yet amplified by differentiation. Our approach addresses both of these problems.

We use a unique set of highly resolved, simultaneous density and direct velocity measurements across the Gulf Stream northeast of Cape Hatteras specifically designed for PV estimation. The data came from a two-ship survey and were obtained as part of the Ph.D. thesis work of Johns (1984). Two ships, one taking CTDs (R/V *Endeavor-087*) and one (R/V *Cape Hat-*

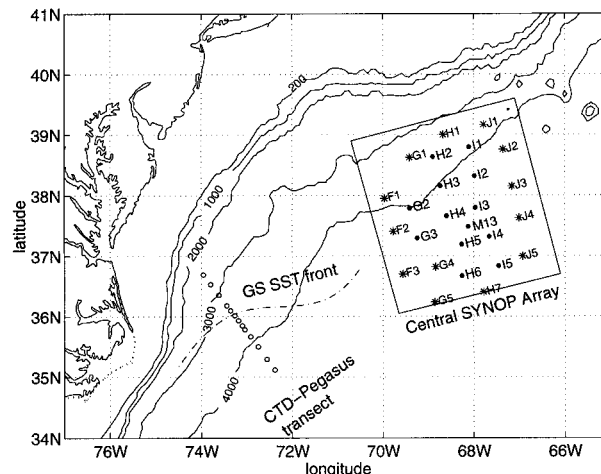


FIG. 1. Study area. The CTD-PEGASUS transect off Cape Hatteras ( $73^\circ\text{W}$ ). Central SYNOP Array: current meter (●) and IES (\*) moorings. Dashed line shows the Gulf Stream SST front position during the survey.

teras-017) deploying PEGASUS instruments (PEGASUS profilers obtain absolute velocity measurements through the water column), were working in close cooperation and in a four-day period completed twice a high-resolution section (shown in Fig. 1) across the Gulf Stream near  $73^\circ\text{W}$ . When the relative vorticity ( $\zeta$ ) becomes of the same order as  $f$  (as is in the Gulf Stream), a simple-scale analysis ( $\zeta \sim f \Rightarrow L \sim V/f \sim 10^4$  m) shows that station spacing ( $L$ ) must be order of 10 km, otherwise  $\zeta$  is underestimated. The data we use had station spacing 12.5 km in the core of the Gulf Stream and 25 km away from the core. CTD measurements extended to the depth of 2 km. NOAA-7 infrared satellite images were obtained for the period of the survey to trace the GS temperature front along-stream in order to account for the curvature vorticity in the PV expression. Johns (1984) and Johns et al. (1989) describe these observations in detail.

In this study we use a PV-gradient (PVG) model to filter out noise from the measured PV and to improve our estimates of the horizontal PV gradients in different layers. The PVG model inverts an input layer PV and returns the depths of the isopycnals (interfaces) and velocities in different layers. The output of the PVG model can be compared against observations, and corrections to an input PV can be made to improve agreement. In this way an idealized and smooth PV-gradient structure can be obtained, which is dynamically consistent with the velocity and density fields and retains the correct magnitudes of the PV gradients, while noise and insignificant details are filtered out.

## 3. Forms of PV: Ertel's and layer

Ertel's potential vorticity  $q$  is expressed (Mueller 1995) as

$$q = \rho^{-1}(\zeta + 2\Omega) \cdot \nabla\psi, \tag{1}$$

where  $\psi$  is a conservative tracer,  $\zeta = \nabla \times \mathbf{U}$ . If the potential density  $\sigma_\theta$  is taken for  $-\psi$  (appropriate for the upper ocean), then (1) yields

$$q = -\rho^{-1} \left[ (\zeta_h \cdot \nabla_h) \sigma_\theta + (\zeta_z + f) \frac{\partial \sigma_\theta}{\partial z} \right], \tag{2}$$

where  $\zeta_h = (-\partial U_y / \partial z, \partial U_x / \partial z)$  is the horizontal component of the relative vorticity,  $\nabla_h = (\partial / \partial x, \partial / \partial y)^T$  is the horizontal gradient operator,  $\zeta_z = \nabla_h \times \mathbf{U}$  and  $f$  are correspondingly the vertical components of the relative and planetary vorticity, with  $z$  axis upward.

We switch to stream coordinates, with the  $x$  axis in the downstream direction and  $y$  increasing to the left, in order to thereby both simplify (2) and obtain a Lagrangian frame moving with the front. An efficient method of coordinate transformation for the Gulf Stream was developed by Halkin and Rossby (1985).

In stream coordinates the downstream component  $\partial \sigma_\theta / \partial x$  is negligible and the first term in (2) simplifies to  $[(-\partial U_x / \partial z)(\partial \sigma_\theta / \partial y)]$ . Given that we know the curvature of the front at the time when the measurements were taken,  $\zeta_z$  can be split into the cross-stream shear component and the curvature vorticity component. This furnishes a practical expression for  $q$ :

$$q = -\rho^{-1} \left[ -\frac{\partial U_x}{\partial z} \frac{\partial \sigma_\theta}{\partial y} + \left( -\frac{\partial U_x}{\partial y} + \kappa U_x + f \right) \frac{\partial \sigma_\theta}{\partial z} \right], \tag{3}$$

where  $\kappa = 1/R$  is the curvature of the front (taken positive for cyclonic meanders and negative for anticyclonic meanders).

In layer models the PV in each layer is expressed (Mueller 1995) as

$$Q_i = \frac{f + \zeta_i}{D_i + \eta_i - \eta_{i+1}}, \tag{4}$$

where  $i$  increases downward,  $D_i$  is the mean layer thickness, and  $\eta_i$  is displacement of an interface between  $i$  and  $i - 1$  layers.

#### 4. Potential vorticity gradient (PVG) model

This section describes a procedure which inverts the prescribed PV (on density surfaces) into the corresponding velocity and density (position of isopycnals) fields.

For the large-scale dynamics, a hydrostatic approximation is used to express the interface displacement through the pressure anomaly,  $P_i$ , vertically averaged within each layer of a multilayer stratified fluid:

$$P_{i+1} - P_i = g \eta_{i+1} (\rho_{i+1} - \rho_i). \tag{5}$$

Here  $\rho_i$  is the vertically averaged potential density in the layer,  $i$  is the layer number increasing downward, and  $\eta_{i+1}$  is the interface displacements between layers  $i + 1$  and  $i$ .

Assuming the flow is stationary and has no variations along-stream, the relative vorticity can be also expressed through the pressure anomaly using the geostrophic relation

$$\zeta_i = -\frac{dV_{xi}}{dy} = \frac{1}{f \rho_i} \frac{d^2 P_i}{dy^2}, \tag{6}$$

where  $V$  denotes geostrophic velocities to distinguish from the measured velocities  $U$  of the previous section.

Combining (4), (5), and (6), we obtain that for a prescribed potential vorticity  $Q_i(y)$ , the geostrophically adjusted pressure anomaly can be found from an elliptic system of equations coupling  $M$  active layers (Sutyrin and Yushina 1989):

$$\begin{aligned} \frac{1}{\rho_i f^2} \frac{d^2 P_i}{dy^2} + \frac{Q_i(y)}{gf} \left( \frac{P_{i+1} - P_i}{\rho_{i+1} - \rho_i} + \frac{P_{i-1} - P_i}{\rho_i - \rho_{i-1}} \right) \\ = \frac{Q_i(y) D_i}{f} \equiv q_i(y) \quad i = 1, 2, \dots, M. \end{aligned} \tag{7}$$

Here  $q_i$  denotes the dimensionless anomaly of the potential vorticity (as in Fig. 4, left panel).

The Gulf Stream front represents a transition area between two water masses with different stratifications which are prescribed by the layer thickness difference between the two sides in each layer. Thus, the potential vorticity on the one side is  $Q_i = f / (D_i - h_i)$ , while on the other side is  $Q_i = f / (D_i + h_i)$ .

In the PVG model we assume that in each layer the potential vorticity changes across the stream in a frontal zone of width  $W_i$ , as

$$q_i = \begin{cases} \frac{D_i}{D_i - h_i}, & \text{for } y \geq Y_i + \frac{\pi W_i}{4}, \\ D_i \left[ D_i - h_i \sin \left( \frac{2(y - Y_i)}{W_i} \right) \right]^{-1}, & \text{for } Y_i - \frac{\pi W_i}{4} < y < Y_i + \frac{\pi W_i}{4}, \\ \frac{D_i}{D_i + h_i}, & \text{for } y \leq Y_i - \frac{\pi W_i}{4}, \end{cases} \tag{8}$$

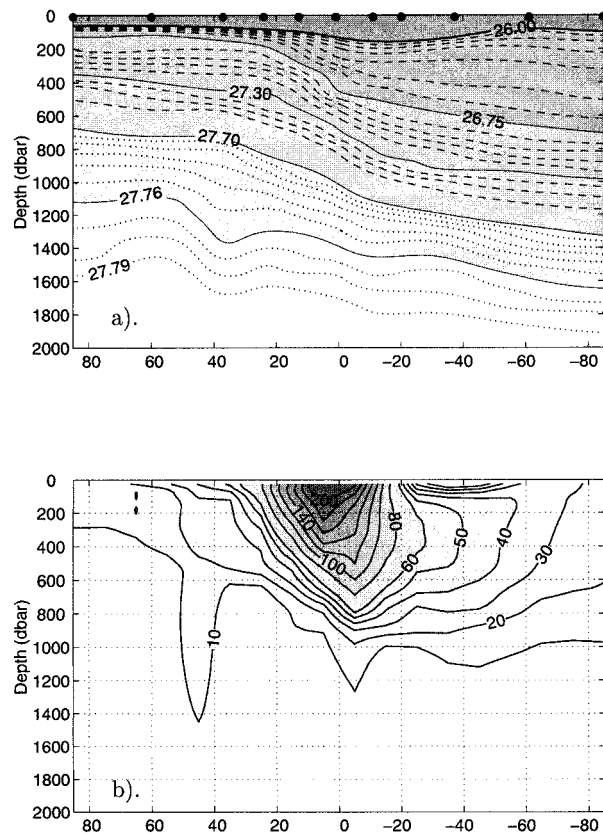


FIG. 2. Measured potential density  $\sigma_\theta$  and downstream velocity  $U_x$  along the CTD-PEGASUS line shown in Fig. 1 (transect 2). (a) Potential density  $\sigma_\theta$ . Bold lines show density layers used in the PVG model. Bullets on top show station positions. (b) Directly measured (PEGASUS) downstream velocity  $U_x$  ( $\text{cm s}^{-1}$ ), relative to 2000 dbar.

where  $Y_i$  is the cross-stream position of the frontal zone.

For  $M$  active layers we assume no motion in the bottom layer ( $P_{M+1} = 0$ ) and a rigid-lid approximation at the surface ( $P_1 = P_0$ ). Corresponding horizontal boundary conditions far from the stream are

$$P_i = \begin{cases} -g \sum_{k=i}^M Z_{k+1}(\rho_{k+1} - \rho_k), & \text{at } y \rightarrow +\infty, \\ g \sum_{k=i}^M Z_{k+1}(\rho_{k+1} - \rho_k), & \text{at } y \rightarrow -\infty, \end{cases} \quad (9)$$

where  $Z_{k+1} = \sum_{l=1}^k h_l$  is the interface depth anomaly.

If  $|q_i - 1| \ll 1$ , the coefficients on the left-hand side of (7) are considered to be independent of horizontal coordinates, so that the solution can be decomposed into vertical modes and expressed analytically. We do not use this (quasigeostrophic) approximation since  $q_i$  ranges from 0 to 10 in the upper Gulf Stream layers. Instead, we use a standard iteration technique (successive over-relaxation) to solve the problem numerically with the boundary conditions (9).

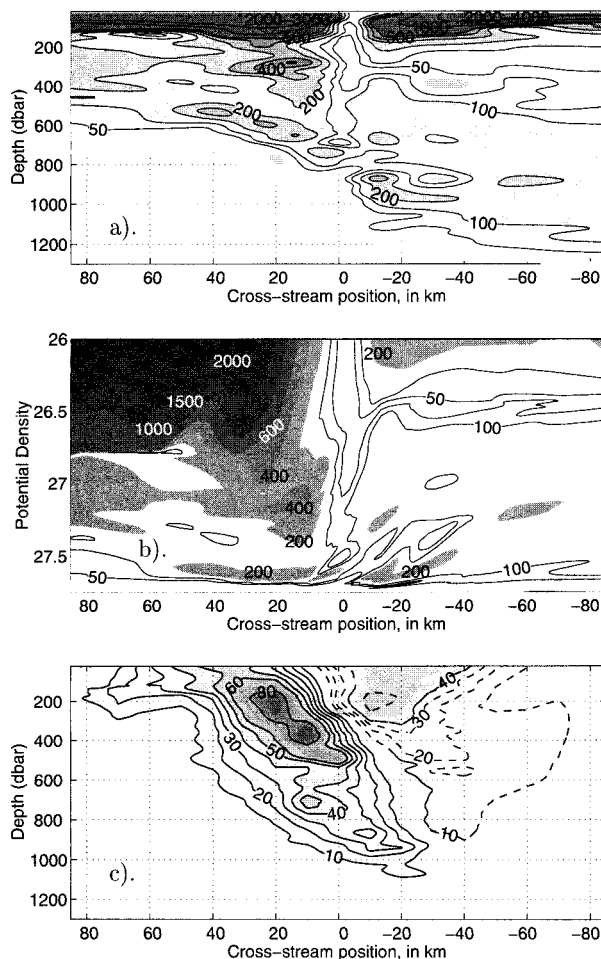


FIG. 3. Ertel's PV as in (3) (units  $10^{-12} \text{ m}^{-1} \text{ s}^{-1}$ ), contoured as a function of (a) depth and (b) density. (c) Relative vorticity component [everything but  $-\rho^{-1} f \partial \sigma_\theta / \partial z$  in (3)], expressed in percent of the planetary PV ( $-\rho^{-1} f \partial \sigma_\theta / \partial z$ ).

## 5. Observed PV

Figures 2a,b show the observed potential density ( $\sigma_\theta$ ) and the downstream component ( $U_x$ ) of the PEGASUS velocities across the Gulf Stream (transect 2). All plots hereafter are given in stream coordinates, and the velocities are taken relative to 2000 m for consistency with the PVG model. Ertel's PV, estimated as in (3) for each of the two transects and then averaged in stream coordinates, is shown in Figs. 3a,b. The derivatives in (3) were estimated from a cubic smoothing spline fitted to the observed  $\sigma_\theta$  and  $U_x$ . Figure 3c shows the relative vorticity component in PV [terms 1, 2, 3 in (3)] expressed in percent of the planetary PV [term 4 in (3)]. As one may see, the relative PV has values greater than 50% of the planetary PV over some portions of the Gulf Stream and must be accurately represented.

As seen in Figs. 3a,b, the surface layer ( $\sigma_\theta < 26.0$ ) has high PV values in summer ( $2000\text{--}4000 \times 10^{-12} \text{ m}^{-1} \text{ s}^{-1}$ ) exceeding by far the PV in the intermediate

and deep layers. However, PV values are subject to seasonal fluctuations in this layer. The underlying 18° Water layer ( $\sigma_\theta = 26.00\text{--}26.75$ , see layer limits in Fig. 2) exhibits a strong cross-stream change in PV. The vast pool of low ( $50\text{--}200 \times 10^{-12} \text{ m}^{-1} \text{ s}^{-1}$ ) PV values on the southern side, associated with weakly stratified Sargasso Sea Mode Water, neighbors a zone of high PV values ( $1000\text{--}2000 \times 10^{-12} \text{ m}^{-1} \text{ s}^{-1}$ ) on the northern side of the stream. The transition zone has a width of about 20 km and is restricted to the upper 700 m ( $\sigma_\theta < 27.3$ ) layer.

A PV minimum occurs on the anticyclonic side (just near the core) of the stream at densities  $\sigma_\theta = 26.0\text{--}27.3$ . Pratt et al. (1991) has employed this minimum to model “warm outbreaks”—anticyclonic warm-core vortices found south of the Gulf Stream. Another feature, a PV maximum on the cyclonic side of the stream at the same density range, was present in both sections (Fig. 3a). The PV maximum is imbedded in the GS density field (see convergence of isopycnals in the  $\sigma_\theta = 26.75\text{--}27.30$  layer, Fig 2a). The PV-gradient sign reversal within this layer satisfies the necessary condition for barotropic instability. The upper Gulf Stream layers ( $\sigma_\theta < 27.3$ ) are mainly responsible for the barotropic instability processes.

Features pertinent to the baroclinic instability of the stream are also seen in Fig. 3a. The horizontal PV-gradient (along isopycnals) reverses sign three times through the water column: from negative in the upper “nonconservative” layer ( $\sigma_\theta < 26.0$ ), to positive in the 18° water layer ( $\sigma_\theta = 26.00\text{--}26.75$ ) and in the upper main thermocline ( $\sigma_\theta > 26.75\text{--}27.30$ ), and back to negative in the layer under the main thermocline ( $\sigma_\theta > 27.70$ ).

## 6. Layer model of the Gulf Stream PV

### a. Layer subdivision

We sought to reproduce the basic Gulf Stream PV structure using the fewest possible layers that still retain essential features of the Gulf Stream structure. The main patterns of Ertel’s PV can be reproduced using the following layer subdivision [we have followed partly the scheme given in Hall and Fofonoff (1993) and retained their terminology and limits when possible].

- 0) The *noninsulated layer* ( $\sigma_\theta < 26.00$ ) is subject to heat and freshwater fluxes from the surface. Ertel’s PV is not conserved in this layer. Due to seasonal variability in PV, we do not include this layer in our PV model because we seek to represent the quasi-permanent Gulf Stream structure.
- 1) The *18° Water layer* ( $\sigma_\theta = 26.00\text{--}26.75$ ) is the layer of strong PV change across the front. The limits were taken such that the PV gradient in the transition zone was approximately of the same value vertically through the layer.
- 2) The *upper main thermocline layer* ( $\sigma_\theta = 26.75\text{--}$

27.30) is the buffer layer between the upper layer (layer 1) with a strong cross-stream PV-change and the underlying layer (layer 3) of nearly uniform cross-stream PV.

- 3) The *main thermocline layer* ( $\sigma_\theta = 27.30\text{--}27.70$ ) is the highly baroclinic layer with nearly uniform cross-stream PV.
- 4) The *lower main thermocline layer* ( $\sigma_\theta = 27.70\text{--}27.76$ ) is the layer of a reversed sign (negative) PV gradient.
- 5) A *quasi-barotropic layer* ( $\sigma_\theta > 27.76$ ) is a very thick deep layer with nearly homogeneous PV (dynamically inactive).

Solid lines in Fig. 2a show this adopted layer subdivision. Layer PV calculated within these layers is given on the left-hand side of Fig. 4. The observed PV contains noise and submesoscale transient features. We used the PVG model to filter out this noise and to improve our estimates of the PV gradients in different layers. The free parameters of the PVG model are listed in Table 1. We sought  $h_i$ ,  $W_i$ , and  $Y_i$  values that reproduce best both the observed PV and the observed velocities within the layers and depths of the interfaces. Since the PVG model is reduced gravity (we use  $4\frac{1}{2}$  layers), the barotropic component (found as a vertical average of velocities in the 1500–2000-m layer) was removed from the direct PEGASUS velocity measurements. We considered a 1-PVG layer and a more refined 3-PVG-layer approximation to the Gulf Stream PV, consistent with observations, and examined what GS velocity features are captured or lost in these PV approximations.

### b. One layer containing a PV gradient (approximation 1)

Observations indicate that the leading order change in PV is associated with the front in the 18° Water layer. Thus, we first used a PV gradient in just one layer, which is the top in Fig. 4. The three other active layers did not contain any PV gradients. Free model parameters  $h_i$ ,  $W_i$ ,  $Y_i$  were adjusted such that all three quantities: PV, velocities, and depths of the interfaces were in good agreement with observations. The values of  $h_i$ ,  $W_i$ ,  $Y_i$  are listed in Table 1.

Figure 4 (right-hand side) shows the observed and model velocities within the layers. The dashed line gives model velocities, which result from a 1-PVG-layer approximation. Maximum velocities are in general well approximated in most of the layers. The width of the stream also closely corresponds to what is observed. Interestingly, the 1-PVG-layer approximation accounts for the asymmetry of the flow, with higher shear on the cyclonic than on the anticyclonic side of the stream. Asymmetry is well reproduced in the PVG layer but not in deeper layers. In the upper layer the Rossby radius of deformation is larger on the anticyclonic side of the

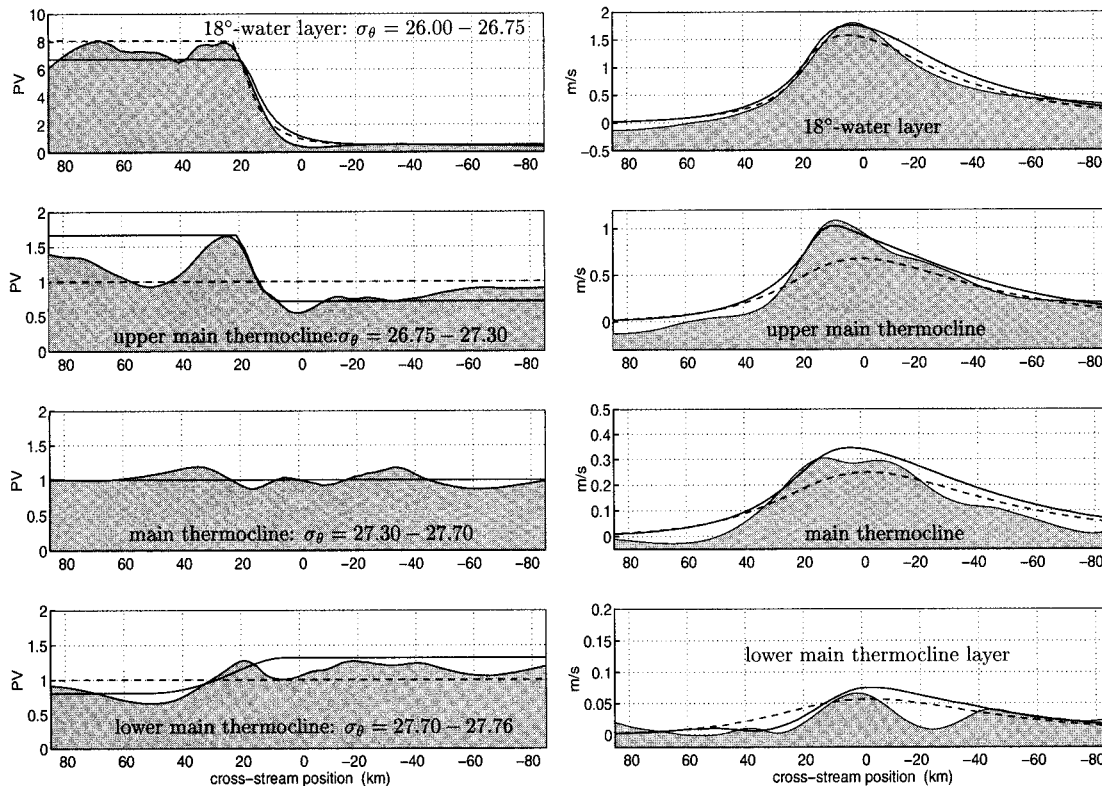


FIG. 4. (Left-hand side) Layer PV (normalized by  $D_i/f$ , where  $D_i$  is the average depth of a layer). Filled plots show the observed PV; solid lines, 3-PVG-layer approximation; dashed lines, 1-PVG-layer approximation. (Right-hand side) Observed and model velocities in density layers; Filled plots, observed velocities; solid lines, velocity reproduced using the 3-PVG-layer approximation; dashed lines, velocity reproduced using the 1-PVG-layer approximation.

Gulf Stream. This causes a lower anticyclonic velocity shear as compared to the cyclonic shear on the opposite side of the stream.

The main discrepancy of the 1-PVG-layer approximation is in the upper main thermocline: velocities in the core of the Gulf Stream are significantly underestimated (see Fig. 4, second panel on the right). Another feature misrepresented is the tilt of the Gulf Stream velocity core toward the anticyclonic side with depth. In the lower main thermocline the core of the Gulf Stream is located farther offshore than in the upper lay-

ers. This tilt is a characteristic feature of the Gulf Stream velocity structure, as is illustrated, for example, in Fig. 5 for Central SYNOP velocity measurements (Johns et al. 1995).

### c. Three layers containing a PV gradient (approximation 2)

The GS velocity features not reproduced in a 1-PVG-layer approximation become well reproduced when two other observed PV patterns are introduced: positive PV

TABLE 1. PVG-model initialization parameters.

| Layer number                              | $i$      | 1                       | 2     | 3     | 4     | 5     |
|-------------------------------------------|----------|-------------------------|-------|-------|-------|-------|
| Potential density                         | $\rho_i$ | 26.37                   | 27.03 | 27.50 | 27.73 | 27.80 |
| Mean thickness (m)                        | $D_i$    | 400                     | 300   | 300   | 330   | 4000  |
| Approximation 1                           |          | One-layer PV gradient   |       |       |       |       |
| Thickness change (m) [defined in Eq. (8)] | $h_i$    | 350                     | 0     | 0     | 0     | 0     |
| Width of the transition zone (km)         | $W_i$    | 30                      | 0     | 0     | 0     | 0     |
| Position of the transition zone (km)      | $Y_i$    | 0                       | 0     | 0     | 0     | 0     |
| Approximation 2                           |          | Three-layer PV gradient |       |       |       |       |
| Thickness change (m) [defined in Eq. (8)] | $h_i$    | 340                     | 120   | 0     | -80   | 0     |
| Width of the transition zone (km)         | $W_i$    | 30                      | 10    | 0     | 30    | 0     |
| Position of the transition zone (km)      | $Y_i$    | 0                       | 15    | 0     | 30    | 0     |

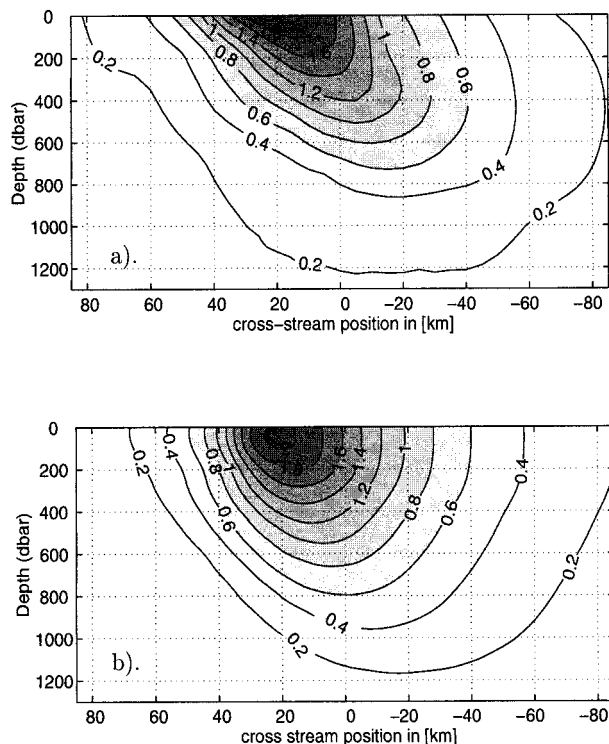


FIG. 5. Comparison against Central SYNOP data: (a) baroclinic velocity structure derived from SYNOP measurements by subtracting the 2000 dbar measured velocities; and (b) model velocities corresponding to the 3-PVG-layer approximation.

gradient in the upper main thermocline and negative in the lower main thermocline. The 3-PVG-layer approximation is shown in Fig. 4 (left-hand side panels, solid lines) with the parameter values listed in Table 1. The corresponding velocity distribution in the layers is given in the right panels (solid lines). It can be compared against the observed baroclinic velocities in the same layers extracted from PEGASUS measurements (filled plots). As one may see, the main discrepancies of the 1-PVG-layer approximation are mended in this 3-PVG-layer model: the core of the Gulf Stream in the upper main thermocline is closely approximated and the tilt of the flow is better reproduced.

## 7. Comparison against SYNOP velocity structure

The PV structure discussed above, although derived from data of only two sections, is characteristic for the Gulf Stream in a mean climatological sense. Because the Gulf Stream PV is relatively stable in time and in space, our results can be used to initialize the mean stream-coordinate Gulf Stream structure and can be projected to a certain extent farther downstream. This can be illustrated, for example, by comparing the PVG model velocities (Fig. 4) against the 2-yr mean velocity structure of the Gulf Stream at 68°W obtained during the SYNOP experiment.

The SYNOP Central Array experiment consisted of a set of current meter and Inverted Echo Sounder deployments with an overall duration over two years, beginning June 1988. The moorings were located along three lines across the Gulf Stream near 68°W (see Fig. 1) and collected data included velocity, temperature, bottom pressure, and sound travel time measurements. Watts et al. (1995) summarize these observations. The SYNOP moored data did not include any salinity measurements (therefore PV could not be estimated directly), but provided a well-resolved depiction of the GS velocity structure. We have used the mean stream-averaged SYNOP velocity data, documented in Johns et al. (1995), to compare against the PVG model velocities.

Figure 5a shows the stream-averaged baroclinic velocities across the Gulf Stream derived from SYNOP measurements (Johns et al. 1995). Figure 5b provides the PVG model velocities, obtained through inversion of the 3-PVG-layer structure. Continuous velocities of Fig. 5b were obtained from layer velocities of Fig. 4 (solid lines) using a cubic spline fit with zero gradient at the surface.

Model velocities have maximum values close to what is observed (about  $2.0 \text{ m s}^{-1}$  in the core), similar width and depth of the stream (about 60 km and 550 dbar correspondingly for velocities  $>1 \text{ m s}^{-1}$ ), and similar values of the horizontal and vertical shear (cyclonic and anticyclonic shear at  $z = 500 \text{ m}$  agree very closely). Note also that the 3-PVG-layer approximation has realistic asymmetry in the velocity structure (higher shear on the cyclonic side than on the anticyclonic), and the core tilts with depth toward the anticyclonic side similar to observations (about 40 km per 1000 dbar).

The main discrepancy between the model and the observed velocities is the absence of the negative vertical shear in the upper layer on the anticyclonic side of model velocities. This negative vertical shear (viz., Fig. 5a) results from advection of the warm core of the Gulf Stream into the colder ambient water. An opposite PV gradient in the surface layer would have been required to capture this feature; however, we do not include the surface layer in our PV model to avoid seasonal fluctuations.

## 8. Summary

A specifically designed set of high-resolution CTD and simultaneous direct velocity measurements were used to estimate Ertel's and layer PV across the Gulf Stream. The PV inversion procedure was implemented to eliminate noise and transient (submesoscale) features from the observed PV and to obtain a simplified but dynamically consistent layer-PV model of the Gulf Stream. Such a layer-PV approximation is required for initialization of a class of numerical and analytical models.

Two approximations to the Gulf Stream PV are of-

ferred and inverted to simulate the Gulf Stream velocity structure. The leading order change in PV is associated with the front in the 18° Water layer. This front alone accounts for the basic velocity structure of the Gulf Stream, including asymmetry of the flow with higher shear on the cyclonic side. The main discrepancy of this 1-PVG-layer approximation arises in the upper main thermocline where the core velocities are considerably underestimated. It also misrepresents the off-shore shift of the core of the stream with depth. Both of these discrepancies are mended by introducing PV gradients in two other layers: positive in the upper main thermocline and negative in the lower main thermocline, consistent with observations. Velocities inverted from this 3-PVG-layer approximation agree well with the 2-yr mean stream-coordinate Gulf Stream structure observed in SYNOP.

*Acknowledgments.* We wish to thank Tom Rossby for kindly sharing with us the PEGASUS directly measured velocity data. We also thank Karen Tracey who assisted in data processing. Financial support was provided by the Office of Naval Research, Contract N000149710138.

#### REFERENCES

- Bane, J. M., Jr., 1980: Coastal-trapped waves in a baroclinic western boundary current. *J. Phys. Oceanogr.*, **10**, 1652–1668.
- Boss, E., N. Paldor, and L. Thompson, 1996: Stability of a potential vorticity front: From quasi-geostrophy to shallow water. *J. Fluid Mech.*, **315**, 65–84.
- Bower, A. S., and M. S. Lozier, 1994: A closer look at particle exchange in the Gulf Stream. *J. Phys. Oceanogr.*, **24**, 1399–1418.
- , H. T. Rossby, and J. L. Lillibridge, 1985: The Gulf Stream — Barrier or blender? *J. Phys. Oceanogr.*, **15**, 24–32.
- Halkin, D., and H. T. Rossby, 1985: The structure and transport of the Gulf Stream at 73°W. *J. Phys. Oceanogr.*, **15**, 1439–1452.
- Hall, M. M., 1994: Synthesizing the Gulf Stream thermal structure from XBT data. *J. Phys. Oceanogr.*, **24**, 2278–2287.
- , and N. P. Fofonoff, 1993: Downstream development of the Gulf Stream from 68° to 55°W. *J. Phys. Oceanogr.*, **23**, 225–249.
- Hoskins, B. J., M. E. McIntyre, and A. W. Robertson, 1985: On the use and significance of isentropic potential vorticity maps. *Quart. J. Roy. Meteor. Soc.*, **111**, 877–946.
- Johns, E., 1984: Geostrophy and potential vorticity in the Gulf Stream northeast of Cape Hatteras, N.C. Ph.D. thesis, University of Rhode Island, Narragansett, RI, 223 pp.
- , D. R. Watts, and H. T. Rossby, 1989: A test of geostrophy in the Gulf Stream. *J. Geophys. Res.*, **94**, 3211–3222.
- Johns, W. E., T. J. Shay, J. M. Bane, and D. R. Watts, 1995: Gulf Stream structure, transport, and recirculation near 68°W. *J. Geophys. Res.*, **100**, 817–838.
- Killworth, P. D., 1980: Barotropic and baroclinic instability in rotating stratified fluids. *Dyn. Atmos. Oceans*, **4**, 143–184.
- Leaman, K. D., E. Johns, and T. Rossby, 1989: The average distribution of volume transport and potential vorticity with temperature at three sections across the Gulf Stream. *J. Phys. Oceanogr.*, **19**, 36–51.
- Liu, M., and T. Rossby, 1993: Observations of the velocity and vorticity structure of Gulf Stream meanders. *J. Phys. Oceanogr.*, **23**, 329–345.
- Lozier, M. S., and D. Bercovici, 1992: Particle exchange in an unstable jet. *J. Phys. Oceanogr.*, **22**, 1506–1516.
- Meacham, S. P., 1991: Meander evolution on quasigeostrophic jets. *J. Phys. Oceanogr.*, **21**, 1139–1170.
- Mueller, P., 1995: Ertel's potential vorticity theorem in physical oceanography. *Rev. Geophys.*, **33**, 67–97.
- Pratt, L. J., and M. E. Stern, 1986: Dynamics of potential vorticity fronts and eddy detachment. *J. Phys. Oceanogr.*, **16**, 1101–1120.
- , J. Earles, P. Cornillon, and J.-F. Cayula, 1991: The non-linear behavior of varicose disturbances in a simple model of the Gulf Stream. *Deep-Sea Res.*, **38** (Suppl. 1A), S591–S622.
- Stommel, H., 1965: *The Gulf Stream: A Physical and Dynamical Description*. University of California Press, 248 pp.
- Sutyrin, G. G., and I. G. Yushina, 1989: Numerical modeling of the formation, evolution, interaction and decay of isolated vortices. *Mesoscale/Synoptic Coherent Structures in Geophysical Turbulence*, J. C. Nihoul and B. M. Jamart, Eds., Elsevier Oceanography Series, Vol. 50, 721–736.
- Watts, D. R., 1983: Gulf Stream variability. *Eddies in Marine Sciences*, A. Robinson, Ed., Springer-Verlag, 114–144.
- , K. L. Tracey, J. M. Bane, and T. J. Shay, 1995: Gulf Stream path and thermocline structure near 74°W and 68°W. *J. Geophys. Res.*, **100**, 18 291–18 312.

